

# Subspace Adaptive Filtering Techniques for Multi-Sensor DS-CDMA Interference Suppression in the Presence of a Frequency-Selective Fading Channel

*Weiping Xu, Michael L. Honig\*, James R. Zeidler†, and Laurence B. Milstein*

Department of Electrical and Computer Engineering

University of California, San Diego

La Jolla, CA 92093-0407

October 28, 1998

## Abstract

The performance of two subspace adaptive filtering techniques for Multi-Sensor DS-CDMA interference suppression is evaluated in the presence of frequency-selective fading. The first technique partially despreads (PD) the received signal, which is coherently combined with an Exponential Least Squares (ELS) adaptive algorithm, a Block Least Squares (BLS) adaptive algorithm, or a MMSE optical filter. The second technique, principal component (PC), projects the received vectors onto an estimated signal subspace obtained by an appropriate eigen-decomposition, which is only coherently combined with a BLS adaptive algorithm.

---

\*Department of Electrical and Computer Engineering, Northwestern University, Evanston, IL 61801

†Space and Naval Warfare Systems Center, Code D8505, San Diego, CA 92152-5001

# 1 Introduction

Linear Minimum Mean Squared Error (MMSE) detection has been proposed to suppress interference for Direct-Sequence (DS) Code-Division Multiple-Access (CDMA) systems [1, 2, 3, 4]. In contrast to nonlinear interference cancellation techniques, linear MMSE detection does not require explicit estimates of interference parameters such as relative amplitudes, phases, and spreading codes. Moreover, it can be implemented as an adaptive tapped-delay line, analogous to linear equalizers for single user channels. MMSE interference suppression has been proposed for multi-carrier receivers [5] and multi-sensor receivers [6] to improve system performance.

In [4], several subspace adaptive linear MMSE detectors for the single sensor DS-CDMA system in a military scenario are considered. The system performances are compared only in the presence of the AWGN channel and under the assumption that power control cannot be used to solve the near-far problem due to peer-to-peer communication. As indicated in [6], a multi-sensor LS adaptive detection can improve system performance if the time-variant channel coefficients of the desired user are known. However, as observed in [7], conventional adaptive algorithms may experience phase slips and false lock with flat Rayleigh fading channels.

Here we employ two subspace adaptive filtering techniques for multi-sensor DS-CDMA interference suppression where the processing gain is large compared with the number of users. The first technique partially despreads the received signal, as proposed in [8]. The second technique, principal component, projects the received vectors onto an estimated signal subspace obtained by an appropriate eigen-decomposition, as proposed in [9, 10]. As the subspace dimension decreases, the response time to interference transients improves; however, the degree of freedom to suppress interferers decreases. The tradeoff is shown by the numerical results. The channel model considered includes a frequency-selective fading, and the adaptive algorithms are presented for the cases of perfect knowledge of the desired user's channel.

The simulation results show that the BLS algorithm is more sensitive to fade rate than are the other addressed algorithm in the paper. The eigen-space projection technique combined with the BLS algorithm performs much better (but is much more complex) than the partial-despreading technique combined with the BLS algorithm when the number of adaptive weights is relatively small. It is also noticed that the multi-sensor structure can significant improve the system performance if the desired user's channel is known.

## 2 System Model

Consider a baseband signal transmitted by the  $k$ th active user as

$$S_k(t) = A_k \sum_{i=-\infty}^{\infty} d_k^{(i)} p_k(t - iT - \tau_k), \quad (1)$$

where  $d_k^{(i)} \in \{\pm 1\}$  is the  $i$ th differentially encoded symbol,  $T$  is the symbol duration,  $\tau_k$  is random time delay uniformly distributed over  $[0, T]$ ,  $A_k$  is the amplitude associated with user  $k$ , and  $p_k(t)$  is a spreading or signature waveform given by

$$p_k(t) = \sum_{n=0}^{N-1} c_k^{(n)} h(t - nT_c), \quad (2)$$

where  $c_k^{(n)} \in \{\pm 1/\sqrt{N}\}$  is the  $n$ th chip of the spreading sequence,  $N$  is the processing gain, which is taken to be equal to the period of the spreading sequence,  $h(t)$  is the chip waveform, and  $T_c$  is the chip duration.

The channel model is assumed to be a frequency selective, Rayleigh channel with  $L$  resolvable paths, and all channels are constant during each symbol interval. The complex low-pass impulse response of the channel for the  $m$ th sensor seen by the  $k$ th user is given by

$$C_{k,m}(t) = \sum_{l=0}^{L-1} \zeta_{k,m,l} \delta(t - lT_c), \quad (3)$$

where  $\zeta_{k,m,l} \equiv \alpha_{k,m,l} \exp(j\beta_{k,m,l})$ , and where the  $\{\alpha_{k,m,l}\}$  are Rayleigh random variables, and the  $\{\beta_{k,m,l}\}$  are uniformly distributed in  $[0, 2\pi]$ . Note that  $\{\zeta_{k,m,l}\}$  are assumed i.i.d for different users  $k$ , different paths  $l$ , and different sensors  $m$ .

The received signal corresponding to the  $m$ th sensor is given by

$$r_m(t) = \sum_{k=1}^K \sum_{l=1}^{L-1} \chi_k \zeta_{k,m,l} S_k(t - lT_c) + n_m(t), \quad (4)$$

where  $\chi_k$  takes on values zero or one, depending on whether or not the  $k$ th interferer is currently transmitting a packet,  $\chi_1 = 1$ , and  $n_m(t)$  is AWGN with zero mean and covariance  $\sigma^2$ .

The structure of  $M$ -sensor receiver is shown in Figure 1, which provides a chip-matched filter for each sensor. letting  $\mathbf{r}_m(i)$  be the  $N$ -vector containing samples at the output of a chip-matched filter for the  $m$ th sensor within the window spanned by  $p_1(t - iT)$ , assuming that the receiver is synchronized to the main path for desired user, say user 1, we can write

$$\mathbf{r}_m(i) = \sum_{k=1}^K \chi_k \{d_k(i) \mathbf{s}_{k,m}^+(i) + d_k(i-1) \mathbf{s}_{k,m}^-(i)\} + \mathbf{n}_m(i), \quad (5)$$

where

$$\mathbf{s}_{k,m}^\pm = \mathbf{P}_k^\pm \mathbf{A}_k \boldsymbol{\zeta}_{k,m}(i), \quad (6)$$

and where

$$\mathbf{P}_k^\pm = [\mathbf{p}_{k,1}^\pm, \mathbf{p}_{k,2}^\pm, \dots, \mathbf{p}_{k,L}^\pm], \quad (7)$$

$$\mathbf{A}_k = \text{diag}[A_{k,1}, \dots, A_{k,L}], \quad (8)$$

and

$$\boldsymbol{\zeta}_{k,m}(i) = [\zeta_{k,m,1}(i), \dots, \zeta_{k,m,L}(i)]'. \quad (9)$$

Note that  $\mathbf{p}_{k,l}^+$  and  $\mathbf{p}_{k,l}^-$  are the vectors of chip-matched filter outputs during symbol  $i$  corresponding to the inputs  $p_k(t - iT - \tau_k - lT_c)$  and  $p_k(t - (i-1)T - \tau_k - lT_c)$ , respectively, which are given in [2] and [3], and  $'$  denotes transpose. The output vectors of the chip-matched filters from  $M$  sensors can be expressed as

$$\mathbf{r}(i) = [\mathbf{r}'_1(i), \dots, \mathbf{r}'_M(i)]'. \quad (10)$$

### 3 Subspace Projection

We consider the situation where the dimension of the received vector  $\mathbf{r}_m(i)$  is greater than the number of (strong) users. In this case, the conventional adaptive filter, where the number of adaptive weights is equal to the processing gain, may not work well in the presence of interference transients, since there are too many *degree of freedom*, which creates very slow convergence modes associated with the noise subspace. As introduced in [4, 10], we can project the received vectors onto a lower dimensional subspace before using any adaptive filtering scheme. Let  $\mathbf{Q}$  be the  $NM \times JM$  projection matrix, where  $J$  is the number of adaptive filter coefficients and  $J < N$ . The projected received vector corresponding to symbol  $i$  is then given by

$$\tilde{\mathbf{r}}(i) = \mathbf{Q}^\dagger \mathbf{r}(i). \quad (11)$$

The output for symbol  $i$  of the adaptive filter with  $JM$  equivalent weights is

$$y(i) = \tilde{\mathbf{w}}^\dagger(i) \tilde{\mathbf{r}}(i). \quad (12)$$

Note that all projected  $JM$ -dimensional quantities are denoted with a *tilde*, and  $\dagger$  represents Hermitian transpose.

### 3.1 Partial Despreading

The received DS-CDMA signal from each sensor is partially despread over consecutive segments of  $I$  chips, where  $I$  is a partial despread rate. The partially despread vector in each sensor has dimension  $J = \lceil N/I \rceil$ , and is the input to the  $J$ -tap adaptive filter in each branch. The projection matrix for  $M$ -sensors is then given by

$$\mathbf{Q} = \text{diag}[\mathbf{q}_1, \dots, \mathbf{q}_M], \quad (13)$$

where  $\mathbf{q}_m$  is the  $N \times J$  projection matrix for each sensor. Note that for the  $M$ -sensor case, all  $\mathbf{q}_m$  are the same for different sensors, since, as described in [4], the columns of  $\mathbf{q}_m$  are non-overlapping segments of the desired spreading sequence, where each segment is of length  $I$ .

### 3.2 Eigen-space Projection

Let  $\mathbf{R} \triangleq E[\mathbf{r}(i)\mathbf{r}^\dagger(i)]$ , be the  $MN \times MN$  covariance matrix for the input vector from  $M$  sensors, and  $\mathbf{x}$  be the steering vector. Since  $\mathbf{R}$  is symmetric and positive semi-definite, we can express it as

$$\mathbf{R} = \mathbf{\Phi}\mathbf{\Lambda}\mathbf{\Phi}^\dagger, \quad (14)$$

where the columns of  $\mathbf{\Phi}$  are the orthonormal eigenvectors, and  $\mathbf{\Lambda}$  is the diagonal matrix of eigenvalues with the assumption that the real-valued eigenvalues satisfy  $\lambda_1 \geq \lambda_2 \geq \dots \geq \lambda_{NM}$ . If we choose the projection matrix as

$$\mathbf{Q} = \mathbf{\Phi}_{1:JM}, \quad (15)$$

where  $\mathbf{\Phi}_{1:JM}$  denotes the  $NM \times JM$  matrix consisting of the first  $JM$  columns of  $\mathbf{\Phi}$ , the reduced-rank filter associated with this projection will be referred to as the *principal components* (PC) filter.

## 4 Adaptive Algorithm

In this section we describe the adaptive algorithms used to estimate the filter coefficients. Three algorithms, the Wiener MMSE solution, the coherent exponential least squares (ELS), and the coherent block least squares (BLS), are combined with partial-despreading, and only the coherent BLS is combined with the eigen-space projection. We evaluate the performance by considering known channel coefficients for the desired user.

## 4.1 Wiener MMSE Solution

With coherent detection the weight vector  $\tilde{\mathbf{w}}(i)$  which minimizes the mean squared error (MSE)  $E(|e(i)|^2)$ , where  $e(i) = d_1(i) - \tilde{\mathbf{w}}^\dagger(i)\tilde{\mathbf{r}}(i)$ , is

$$\tilde{\mathbf{w}}(i) = \tilde{\mathbf{R}}^{-1}(i)\tilde{\mathbf{x}}(i), \quad (16)$$

where

$$\begin{aligned} \tilde{\mathbf{R}}(i) &\triangleq E[\tilde{\mathbf{r}}(i)\tilde{\mathbf{r}}^\dagger(i)] \\ &= \mathbf{Q}^\dagger \mathbf{R}(i)\mathbf{Q}, \end{aligned} \quad (17)$$

$$\begin{aligned} \mathbf{R}(i) &\triangleq E[\mathbf{r}(i)\mathbf{r}^\dagger(i)] \\ &= \sum_{k=1}^K \chi_k [\mathbf{s}_k^+(i)(\mathbf{s}_k^+(i))^\dagger + \mathbf{s}_k^-(i)(\mathbf{s}_k^-(i))^\dagger] + \sigma_n^2(i)\mathbf{I}, \end{aligned} \quad (18)$$

and

$$\begin{aligned} \tilde{\mathbf{x}}(i) &\triangleq E[d_1(i)\tilde{\mathbf{r}}(i)] \\ &= \mathbf{Q}^\dagger \mathbf{s}_1^+(i), \end{aligned} \quad (19)$$

Where  $\mathbf{Q}$  can be any projection matrix. Note that Eqn. (18) is obtained based on the assumption of known channel for desired user and trackable channel for multiple access interferer.

## 4.2 Exponential Least Square

We use the ELS algorithm combined with partial despreading for the multi-sensor DS CDMA receiver. The ELS algorithm is given by [11],

$$\hat{\tilde{\mathbf{R}}}(i+1) = (1 - \epsilon)[\tilde{\mathbf{r}}(i)\tilde{\mathbf{r}}^\dagger(i)] + \epsilon\hat{\tilde{\mathbf{R}}}, \quad (20)$$

and

$$\tilde{\mathbf{w}}(i+1) = \hat{\tilde{\mathbf{R}}}^{-1}(i+1)\tilde{\mathbf{x}}(i+1), \quad (21)$$

where the steering vector  $\tilde{\mathbf{x}}(i+1)$  in Eqn. (21) is given by Eqn. (19) for a known channel model.

## 4.3 Block Least Squares

The BLS algorithm obtains the covariance matrix by time-average instead of the ensemble-average for MMSE. It can then be predicted that the algorithm should work well in a AWGN channel. The

simulation results confirm that it only works well in a very slow fading channel relative to the block length,  $B$ , which is an important parameter affecting the error rate in the presence of time-varying fading. The time-averaged covariance matrix is given by

$$\hat{\mathbf{R}}(i) = \frac{1}{B} \sum_{j=i-B+1}^i \mathbf{r}(j)\mathbf{r}^\dagger(j), \quad (22)$$

and for a known channel assumption, the estimate of steering vector is given by

$$\hat{\mathbf{x}}(i) = \frac{1}{B} \sum_{j=i-B+1}^i \mathbf{s}_1^+(j). \quad (23)$$

The projection matrix  $\mathbf{Q}$  for the BLS algorithm can be obtained corresponding to the two projection techniques described in Section 3.

## 5 Numerical Results

The main parameters chosen for simulation are following: The processing gain is  $N = 64$ , and there are three asynchronous users. The received power of interferers varies with the standard deviations of  $1.5dB$ . All received signals experience a 2-path Rayleigh fading, and relative power loss of each path to main path is  $3dB$ . The signal-to-noise ratio is  $1/\sigma_n^2 = 9dB$  per path for each sensor. Note that, for the complex Gaussian noise,  $N_0 = 2\sigma_n^2$ . Each curve is obtained by averaging 20 runs and 10,000 symbols per run.

### 5.1 Effect of the Partial Despreading Factor $I$

The performance comparison between one sensor system and two sensor system is first shown in Fig. 2 for ELS and MMSE algorithms combined with partial despreading technique respectively, where the adaptive filter coefficients are updated every symbol. The normalized Doppler frequency of  $f_d T \approx 0.00035$  cycles/symbol. However, in practice, mobile users experience different fade rates, which depend on velocities.

Two parameters for the adaptive algorithms are the exponential weighting factor, which is set as  $\epsilon = 0.995$  (corresponding to an averaging window length of approximately  $1/(1 - \epsilon) = 200$  symbols), and the training period, which is set as 200 symbols to acquired the desired user in the simulation. The initial values of  $\hat{\mathbf{R}}$  and  $\hat{\mathbf{x}}$  are taken to be  $0.01 \times \mathbf{I}$  and the vector of zeros, respectively. Performance is relatively insensitive to this choice. The subspace dimension is  $J = \lceil N/I \rceil$ . The curves with diamond mark correspond to the two-sensor receiver and the various line

styles correspond to the different algorithms. It is shown from the figure that the two-sensor system can offer a significant improvement in performance relative to the one-sensor system, and the MMSE filter always outperforms the ELS algorithm. There is a obvious degradation in performance for MMSE as the partial despreading factor increases, i.e., the subspace dimension decrease, which means that the degree of freedom to suppress interference decreased. However, we cannot observe such degradation for ELS algorithm.

With the same parameters as used in Fig. 2, the performances are compared for the BLS algorithm combined with partial despreading technique or principal component subspace technique, where the adaptive filter coefficients are updated every block, and the subspace dimension is  $J = \lceil N/I \rceil$ . The performance improvement of the two sensor system is obvious too. It is also shown that the eigen-space algorithm can offer a significant improvement in performance relative to partial despreading for a large partial despreading factor, but with a significant increase in computational complexity (i.e., an eigen-decomposition is required for each block).

## 5.2 Effect of Fading Rate

Figure 4 shows the effect of fading rate on the system performances for ELS algorithm, BLS algorithm, and MMSE filter combined with partial despreading respectively, where we use the same parameters as used in Figure 2 besides that we fixed the partial despreading factor as  $I = 8$ , i.e.,  $J = 8$ . It is shown that all the algorithms always benefit from an increase in sensors. Additional, the BLS algorithm is more sensitive to the mobile speed than both MMSE and ELS algorithms. This is because the BLS algorithm updates filter coefficients every block. The higher the Doppler shift, the more difficult for the BLS algorithm to estimate the time-varying steering matrix within a block even such estimation is based on the known channel coefficient for each symbol.

The effect of a mobile speed is also shown by Figure 5 for the BLS algorithm combined with partial despreading technique or principal component subspace technique, where we use the same parameters as used in Figure 4. Although the BLS algorithm is sensitive to the mobile speed, the improvement in performance by increasing the number of sensors is still true. It is also shown that when the subspace dimension, say 8, close to the strong interferers in the system, 6, the BLS algorithm associated with the eigen-space decomposition can achieve the better performance than the BLS algorithm associated with partial despreading.

## 6 Conclusions

The performance of subspace adaptive filtering techniques for multi-sensor DS-CDMA in the presence of a frequency-selective fading has been studied. A comparison is made by simulation for a single-sensor receiver structure and a two-sensor receiver structure. The results indicate that all the algorithms can always benefit from the two-sensor structure. The MMSE filter achieves the best performance when subspace dimension is large relative to the number of interferers. It is also noted from the results that the principal component subspace technique will outperform other algorithm addressed in the paper when subspace dimension is small relative to the number of interferers. Finally, The block-oriented LS algorithms is more sensitive to the fading rate (mobile speed) than non-block-oriented algorithms.

## References

- [1] Rapajic and B.S. Vucetic, "Adaptive Receiver Structures for Asynchronous CDMA Systems", *IEEE JSAC*, vol. 12, no. 4, pp. 685-697, May 1994.
- [2] U. Madhow and M. L. Honig, "MMSE interference suppression for direct-sequence spread-spectrum CDMA," *IEEE Trans. on Comm.*, vol. 42, pp. 3178-3188, Dec. 1994.
- [3] S. L. Miller, "An adaptive direct-sequence code-division multiple-access receiver for multiuser interference rejection", *IEEE Trans. on Comm.*, vol. 43, No. 2/3/4, pp. 1746-1755, Feb.-April 1995.
- [4] M. L. Honig, "A comparison of subspace adaptive filtering techniques for DS-CDMA interference suppression," *Proc. MILCOM'97*, vol. 2, pp. 836-840, Nov. 1997.
- [5] W. Xu and L. B. Milstein, "MMSE Interference Suppression for Multicarrier DS-CDMA in Frequency Selective Fading Channels", *Submitted to Globecom'98*.
- [6] S. Buljore, M.L. Honig, J. Zeidler, and L.B. Milstein, "Adaptive Multi-sensor Receivers for Frequency Selective Channels in DS-CDMA Communications Systems", *Proc. 31st Asilomar Conf. on SSC*, Nov. 1997.
- [7] A. N. BARbosa and S. L. Miller, "Adaptive Multiuser Detection of DS-CDMA signals in fading channels", *IEEE Trans. comm.*, vol. 46, no. 1, pp. 115-124, Jan. 1998.
- [8] R. Singh and L. B. Milstein, "Adaptive interference suppression for Direct-Sequence CDMA," *Submitted to IEEE Trans. on Comm.*

- [9] J. S. Goldstein and I. S. Reed, "Reduced-Rank Adaptive Filtering" *IEEE Trans. on SP*, Vol. 45, No. 2, pp. 492-496, Feb. 1997.
- [10] X. Wang and H. V. Poor, "Blind Multiuser Detection: A Subspace Approach", *IEEE Trans. on IT*, Vol. 44, Num. 2, pp. 677-690, Mar. 1998.
- [11] M. L. Honig, S. L. Miller, M. J. Shensa, and L.B. Milstein, "Performance of Adaptive Linear Interference Suppression in the Presence of Dynamic Fading", *submitted to IEEE Trans. Comm.*
- [12] S. E. Bensley and B. Aazhang, "Subspace-BAsed Channel Estimation for CDMA Communication Systems", *IEEE Trans. Comm.*, vol. 44, no. 8, pp. 1009-1020, Aug. 1996.

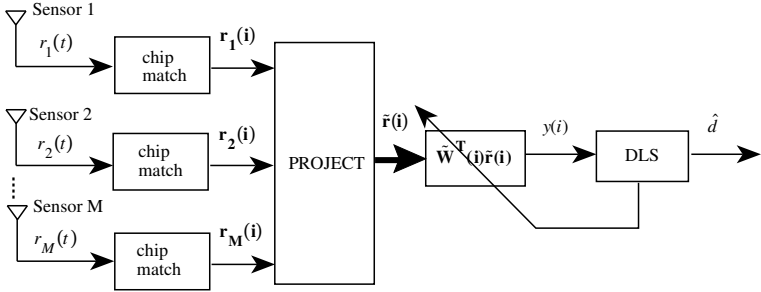


Figure 1: Multi-sensor Baseband Receiver Block Structure for User 1

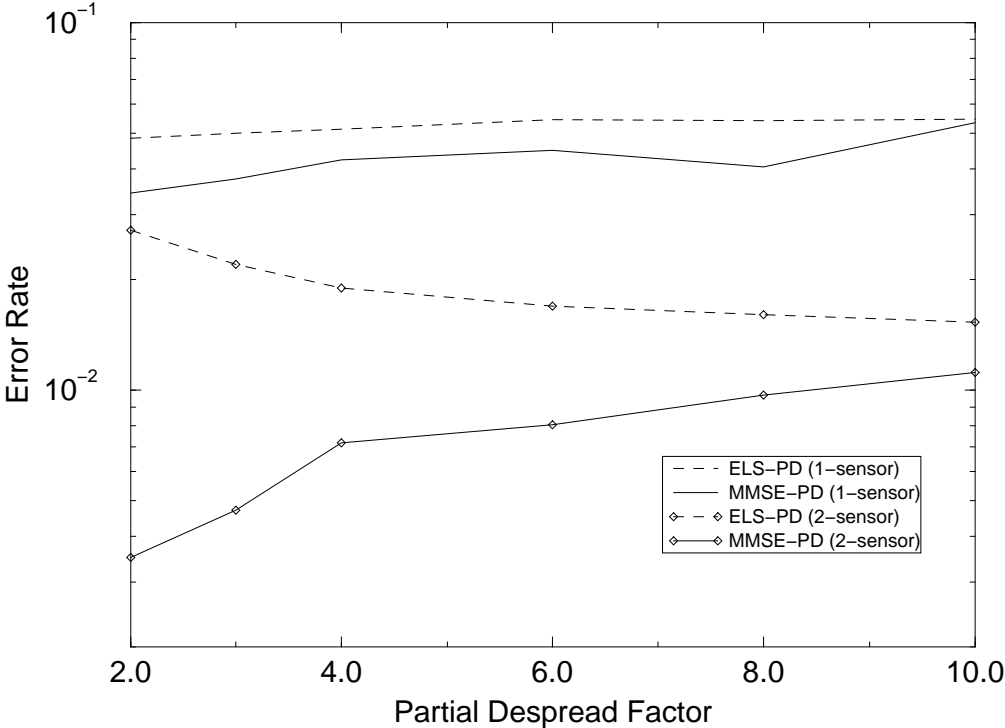


Figure 2: Error rate vs. partial despreading factor  $I$  for a 2-path Rayleigh fading channel.  $N=64$ , 3 users with the standard deviation of power 1.5dB for each path,  $1/f_d T \approx 2863$  symbols/fade cycle (speed=5 mph),  $1/\sigma_n^2 = 9$ dB per path.

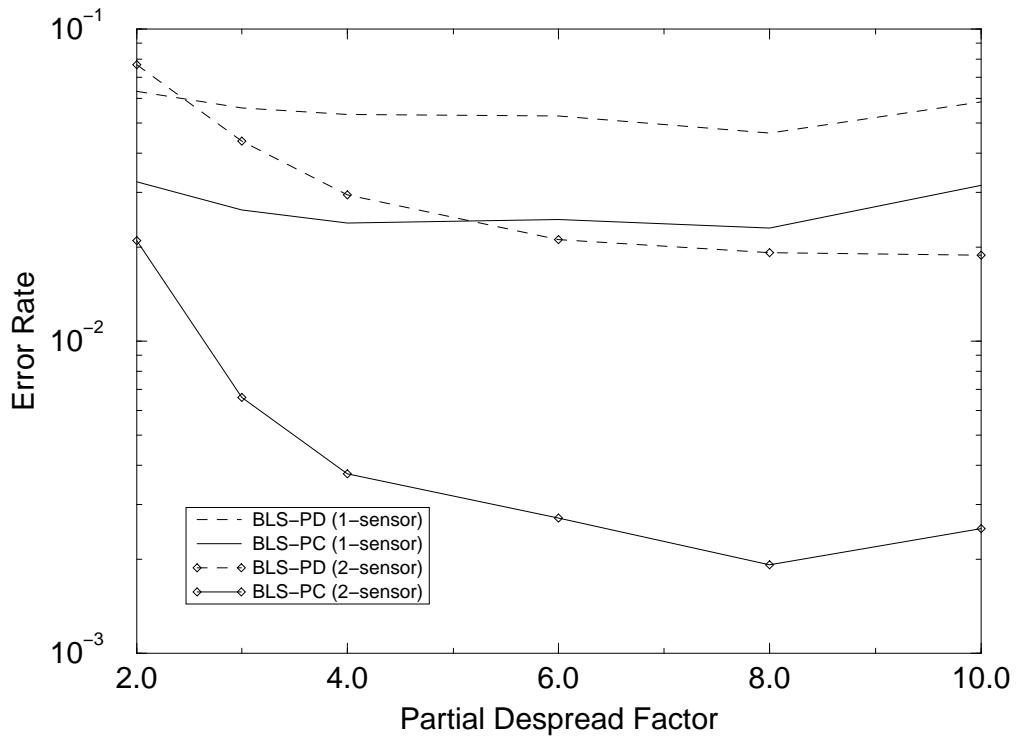


Figure 3: Error rate vs. partial despreading factor  $I$  for a 2-path Rayleigh fading channel.  $N=64$ , 3 users with the standard deviation of power 1.5dB for each path,  $1/f_d T \approx 2863$  symbols/fade cycle (speed=5 mph),  $1/\sigma_n^2 = 9$ dB per path.

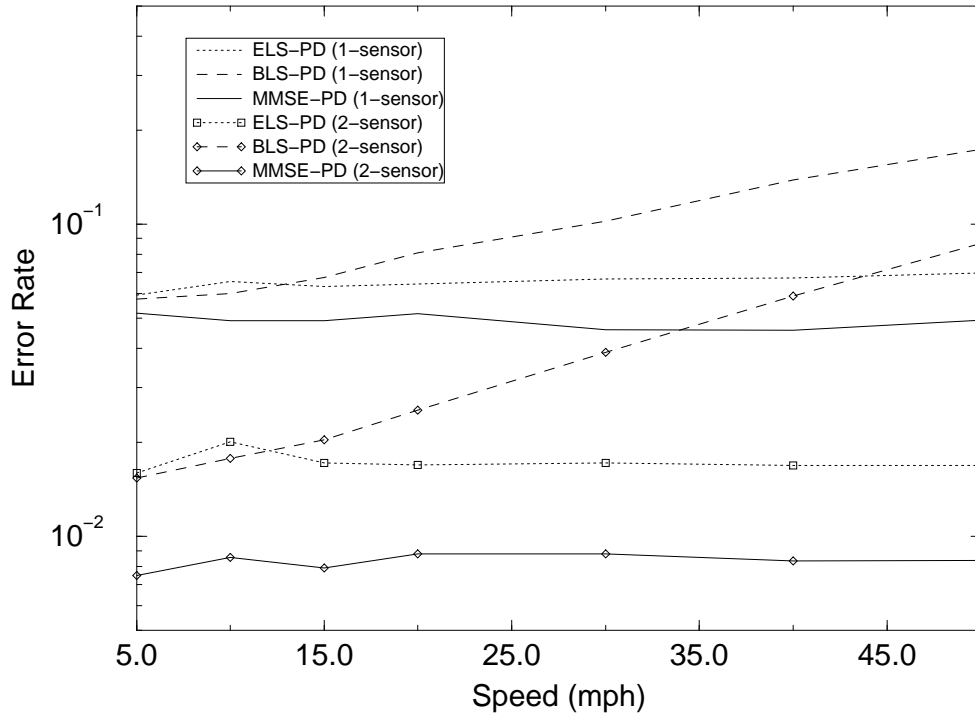


Figure 4: Error rate vs. mobile speed (mph) for a 2-path fading channel.  $N=64$ ,  $J=8$  ( $I=8$ ), 3 users with the standard deviation of power 1.5dB for each path,  $1/\sigma_n^2 = 9\text{dB}$  per path.

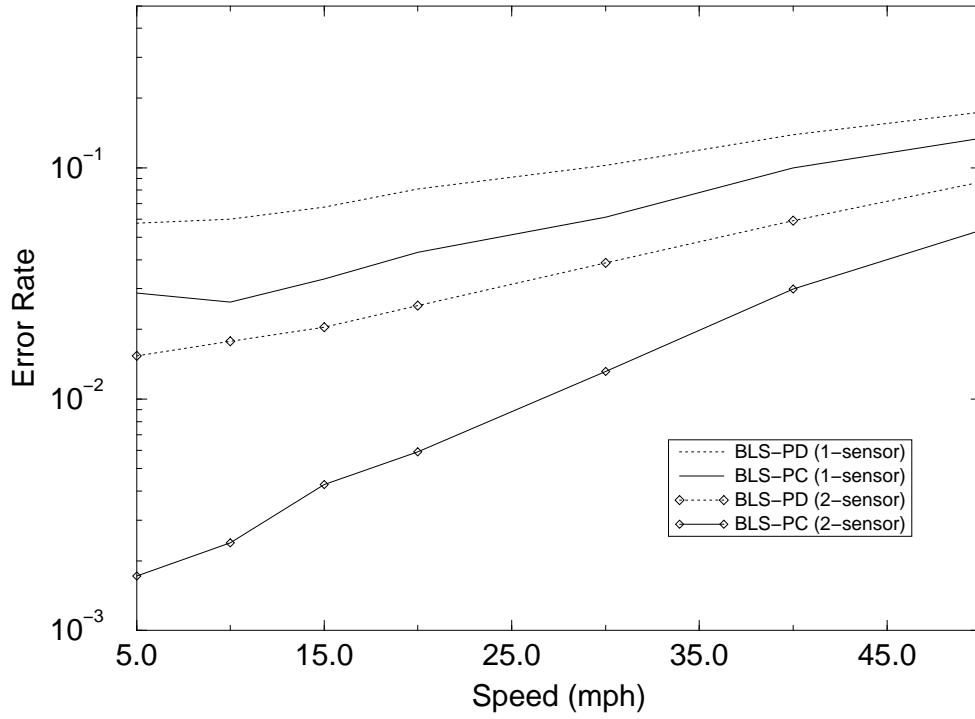


Figure 5: Error rate vs. mobile speed (mph) for a 2-path fading channel.  $N=64$ ,  $J=8$  ( $I=8$ ), 3 users with the standard deviation of power 1.5dB for each path,  $1/\sigma_n^2 = 9$ dB per path.